ABSORPTION, PHOTOLUMINESCENCE AND RAMAN SPECTRA OF SOME SULFIDE AND TELLURITE/HALIDE GLASSES

M. Ožvoldová[a], V. Trnovcová[a,b*], M. Kadlečíková[c], A. Škubla[a], J. Greguš[d], J. Zavadil[e], D. Ležal[f]

[a]Faculty of Materials Science and Technology, Slovak University of Technology, SK-91 724 Trnava, Slovakia
[b]Institute of Physics, Slovak Academy of Sciences, SK-84228 Bratislava, Slovakia
[c]Slovak University of Technology, Microelectronics Department, SK - 812 19 Bratislava, Slovakia
[d]Faculty of Mathematics and Physics, Comenius University, SK-82415 Bratislava, Slovakia
[e]Institute of Radio Engineering and Electronics, Academy of Sciences of Czech Republic, CZ - 182 51 Praha, Czech Republic
[f]Laboratory of Inorganic Materials, Institute of Inorganic Chemistry, Academy of Sciences of Czech Republic & Institute of Chemical Techology, CZ-166 28 Prague, Czech Republic

Absorption, luminescence and Raman spectra of $Ge_{25}Ga_{10}S_{65}$, $Ge_{25}Ga_5As_5S_{65}$, and 70 $TeO_2 \cdot$ 30 $PbCl_2$ glasses doped with Pr^{3+} ions in various concentrations and chemical forms are measured and analyzed. The $Ge_{25}Ga_{10}S_{65}$ and $Ge_{25}Ga_5As_5S_{65}$ glasses seem to be the best glass matrices for the Pr^{3+} photoluminescence at 1.32 μm. Their energy level diagrams and amplifying mechanisms of Pr^{3+} ions are described. Their phase transition temperatures are detected and an optimum fiber drawing temperature is proposed.

1. Introduction

Silica glass optical fibers for telecommunications mostly operate at 1.31 μm because the group velocity zero dispersion point falls around this wavelength. Due to intrinsic scattering and absorption processes, an amplification of the signal is required. Therefore, optical fiber amplifiers working in this spectral region are of a major importance. Some of rare earth ions (Pr, Nd, Dy) have relatively long-lived metastable states which decay by emission of the radiation around this wavelength. However, these rare earth ions have a low solubility in silica glasses. A development of a suitable glass matrix, having a low phonon energy, a higher value of the refraction index, high chemical and physical purity and a sufficient solubility of rare earth (RE) ions, and being transparent at the pump and signal wavelengths, is needed. Fluoride, chalcogenide and heavy metal oxide (HMO) glasses seem to be promised host materials for these amplifiers [1-4].

When fluoride, chalcogenide or HMO glass fibers are doped with suitable rare earth ions, a telecommunication signal can be amplified by means of their stimulated emission, upon optical pumping by a laser diode [5-7]. Due to higher pump power efficiency, germanium sulfide glasses are the most promising hosts for fiber amplifiers [3]. An addition of Ga_2S_3 to these glasses increases the solubility of rare earth ions. A significant improvement of the stability of Ge-Ga-S glasses is obtained by adding the most prominent glass former, As_2Se_3.

---

* Corresponding author: fyzitrno@mtf.stuba.sk

This paper presents the absorption, photoluminescence and Raman spectra of the $Ge_{25}Ga_{10}S_{65}$ (GGS), $Ge_{25}As_5Ga_5S_{65}$ (GAGS) and $70\ TeO_2\cdot30\ PbCl_2$ (TPO) glasses doped with Pr^{3+} ions in various concentrations and chemical forms. The results are discussed from the point of view of the microstructure, of the fiber drawing ability and of the amplifying schemes. Dominant structural units in the glasses are specified. For the most suitable glass ($Ge_{25}Ga_{10}S_{65}$), the temperatures of glass formation (T_g), crystallization (T_x), and undercooled liquid state (T_{ULS}) are determined. From these temperatures an optimum fiber-pulling temperature is estimated.

2. Experimental

The $Ge_{25}Ga_{10-x}RE_xS_{65}$ (GGS), $Ge_{25}As_5Ga_{5-x}RE_xS_{65}$ (GAGS), and $70\ TeO_2\cdot 30\ PbCl_2$ (TPO) glasses were used in our experiments. The glasses were doped with 500 to 3000 wt-ppm Pr^{3+} (nominal concentrations). The Pr^{3+} ions were added as chlorides, sulfides, oxides or in elemental form.

All technological procedures were done in one special quartz ampoule as to lower the contamination during the preparation [8,9]. The presence of OH^- groups induces a development of clusters and decreases the solubility of rare earth elements. The necessary chemical and physical purity of glasses should be of about 10^{-5} m/o OH^- (SH^-) impurities and 10^2-10^3 cm^{-3} physical defects. Therefore, a purification of starting materials is necessary. Sublimation under vacuum and the reactive atmosphere are effective for purification of As, Ge, S, Te. A melting under vacuum is effective for purification of Ge and Ga. The melting temperature of sulfide glasses depends on their composition (700-950 ^{o}C). The melting times are 15-20 hours and then the ampoule with a glass melt was cooled to room temperature. Prepared glasses were annealed about 10 ^{o}C below the glass transition temperature (T_g) as to relieve thermal stresses.

Before the synthesis of TPO glasses, all starting compounds were dried under vacuum (230 ^{o}C, 5 hours), under a flow of oxygen and in a reactive chlorine atmosphere (obtained by a decomposition of CCl_4 at 800 ^{o}C) in order to remove moisture from their surface. A subsequent melting was carried out for 30 min. at 720 ^{o}C. Subsequently, the glass melt was poured into forms (ϕ7 mm x 40 mm) and annealed slowly from T_g to room temperature (RT).

Absorption and transmission spectra were measured in the ultraviolet, visible and near infrared spectral regions (200-3000 nm) by using Specord UV-VIS spectrometer and Specord 61 NIR spectrometer. The emission spectra were detected by a standard system with a lock-in amplifier and Si or Ge photodiodes. For the excitation of GGS and GAGS glasses, a semiconductor laser of 807 nm and a He-Ne laser (632.8 nm) were used. For the excitation of TPO glasses, a semiconductor laser of 807 nm and the He-Cd laser of 325 nm were used. Spectra were recorded with a spectral resolution of about 1nm using a single grating Zeiss monochromator, in the range of 800-1500 nm. Measurements at RT were performed.

Raman measurements were made using Raman spectrometer Dilor-Jobin Yvon-Spex, type LabRam. The excitation source is a He-Ne laser (632.8 nm). The spectral range is from 450 nm to 1050 nm. The air-cooled CCD detector has a resolution better than 1.3 cm^{-1}. The measurements were carried out at room temperature. The lateral resolution is 1 μm. Under these conditions,   also a photoluminescence in the spectral ranges of 500-620 nm and 640- 900 nm was measured.

For DSC measurements, DSC-7, Perkin-Elmer, Al pans and Ar atmosphere were used. The accuracy of temperature data is $\pm$0.5 K. For the GGS and GAGS glasses, the values of T_g, T_{ULS}, and T_x were determined. The values of T_g and T_x are the onset ones. For each sample, two heating cycles (up to 600 ^{o}C, at a heating rate, v, of 20 ^{o}C/min and 10 ^{o}C /min) were done.

3. Results

3.1. Optical properties

3.1.1. Absorption spectra

Seven absorption bands due to optical transitions from $^3H_4$ level in Pr^{3+} ion have been detected and identified in the GGS and GAGS glasses (Table 1). Up to 3000 wt-ppm Pr^{3+}, the energies are

independent of the Pr^{3+} concentration and of its chemical form. Both in the GGS and GAGS glasses, the same ground state absorption transitions were observed.

The absorption edge of TPO glass and the influence of Pr^{3+} doping on the edge are shown in Fig. 1. The short wavelength absorption edge is located at 429 nm. A step at this edge, probably connected with the $PbCl_2$ component, was observed. This step is more distinct in doped glasses. Upon doping, the sharpness of this edge decreases, and at higher concentrations of dopant (> 1000 wt-ppm), the edge is shifted to shorter wavelengths (419-424 nm).

In the TPO glass, only six absorption bands due to optical transitions from $^3H_4$ level of Pr^{3+} ion have been detected (Table 1). In comparison to sulfide glasses, these levels are significantly shifted to higher energies. Dominant absorption bands are at 5128 and 6457 cm^{-1}. However, these bands were not observed upon doping with Pr_2O_3.

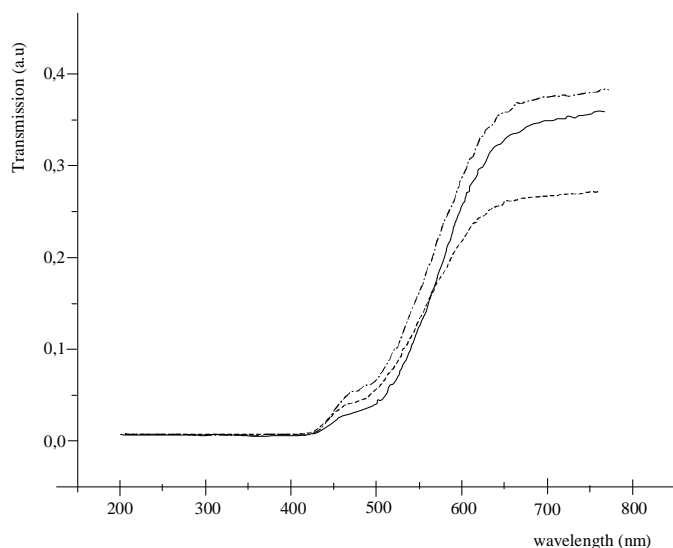Fig. 1. A short wavelength absorption edge in TPO (full line), TPO:1000 ppm Pr^{3+} (dashed line) and TPO:2000 Pr^{3+} (dashed and dotted line) glasses.

Table 1. Absorption bands due to optical transitions from $^3H_4$ level in Pr^{3+} in the GGS, and GGAS glasses, and in TPO ones.

Assignment [Pr^{3+}]	Energy [cm^{-1}] (GGS, GGAS)	Energy [cm^{-1}] (TPO)
$^3H_6$	4 250	4444
$^3F_2$	4 920	5128
$^3F_3$	6 270	6457
$^3F_4$	6 708	6897
$^1G_4$	9 700	10981
$^1D_2$	15 873	14084 ?
$^3P_0$	19 607	21740

3.1.2. Photoluminescence spectra

In Fig. 2 a,b,c, three bands of the photoluminescence spectrum (at RT) of the GGS glass doped with 1000 wt-ppm Pr^{3+} (added as a sulfide) are presented. The shape of the spectrum and wavelengths of individual peaks are very close to those of the glasses doped with Nd^{3+} [10]. In the spectral region from 0.85 to 0.95 μm, two peaks correspond to the $(^3P_o, {}^3P_1) \rightarrow {}^1G_4$ transitions. In the spectral region

from 1.03 to 1.115 μm, two peaks correspond to the $^1D_2\rightarrow(^3F_4,{}^3F_3)$ transitions. In the spectral region from 1.3 to 1.44 μm, three peaks correspond to the $^1G_4\rightarrow{}^3H_5$ transitions. Up to 3000 wt-ppm Pr^{3+}, the concentration quenching is low. The proposed schematic energy level diagram is presented in Fig. 2d.

In Fig 3 a,b,c, photoluminescence spectra of TPO glasses doped with various concentrations of Pr^{3+} ions are shown in the ranges 500-620 nm and 640-920 nm. In the range of 500-620 nm, only one band, at approximately 613.5 nm is observed both in pure glasses and in glasses doped with Pr_2O_3. Upon Pr^{3+} doping, this band was shifted to 604 nm. In the range 640-920 nm, a photoluminescence peak at 642 nm, a splitted peak 660/662 nm and a broad band around 796 nm are present in "pure" TPO glass. A similar spectrum is observed also upon doping with Pr_2O_3. Upon Pr^{3+} doping, the intensity of the peak at 660 nm is enhanced and increases with increasing concentration of Pr^{3+}. A new PL double band appears with peaks at 869 and 877 nm. For Pr^{3+} concentrations higher than 1000 wt-ppm, a concentration quenching of this photoluminescence is observed. At longer wavelengths, we have not observed any photoluminescence under our excitation conditions.
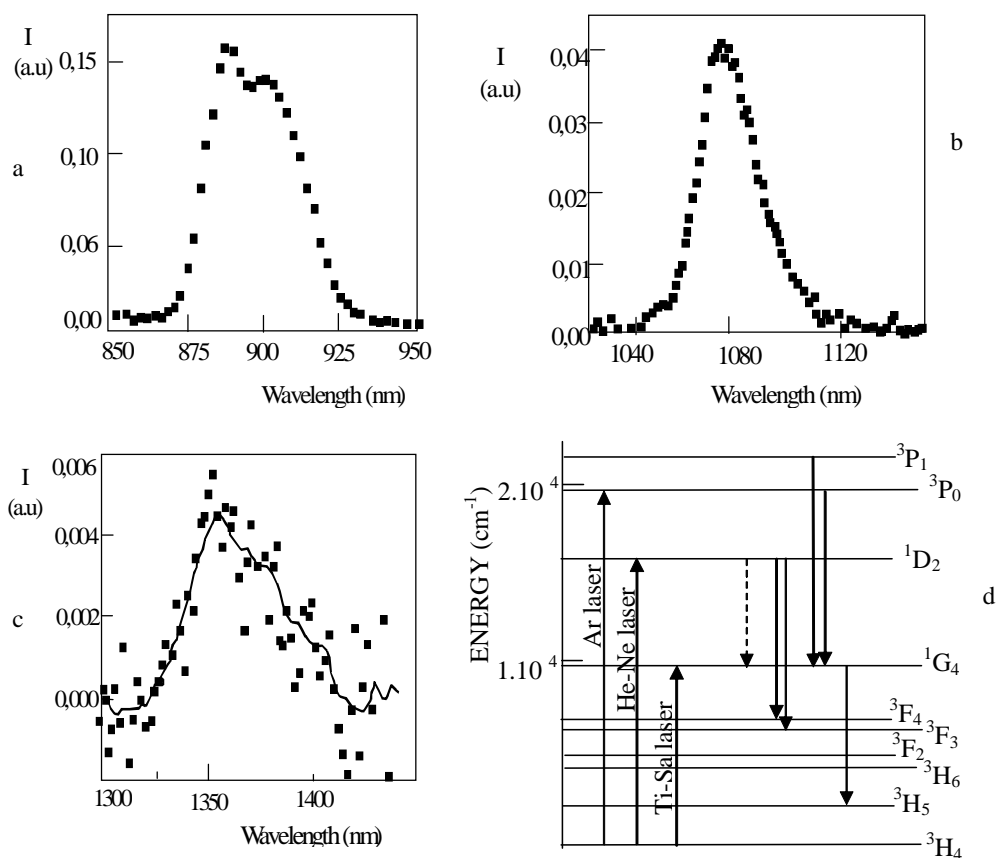

Fig. 2. a,b,c. Photoluminescence spectrums of the GGS:1000 wt-ppm glass(at RT) in various spectral regions, d. Energy level diagram of Pr^{3+} ion with observed 4f-4f inner shell radiative and pump transitions.

3.1.3. Raman scattering

In Fig 4 a,b, Raman spectra of the Ge-Ga-S and Ge-Ga-As-S glasses, doped with different rare earth ions, are shown. Measurements of different areas of samples confirmed a homogeneity of glasses. There was no influence of dopants on the Raman spectra and homogeneity of both glasses.In Fig. 5, Raman spectrum of the TBO glass is presented. No influence of a Pr^{3+} doping on the spectrum was observed. Four bands were observed upon He-Ne laser excitation at RT. They are centered at 320, 445, 659, and 708 cm^{-1}. The peak at 708 cm^{-1} is dominant.

3.2. Phase transitions

In Fig. 6 a, a differential thermogram of the $Ge_{25}Ga_{10}S_{65}$ glass is presented. The value of T_g is equal to 436.7 ^{o}C. The transformation region ends at 499.6 ^{o}C (T_{ULS}). The T_x value is equal to 588.8 ^{o}C. The value of the crystallization enthalpy is equal to 117 J/g.
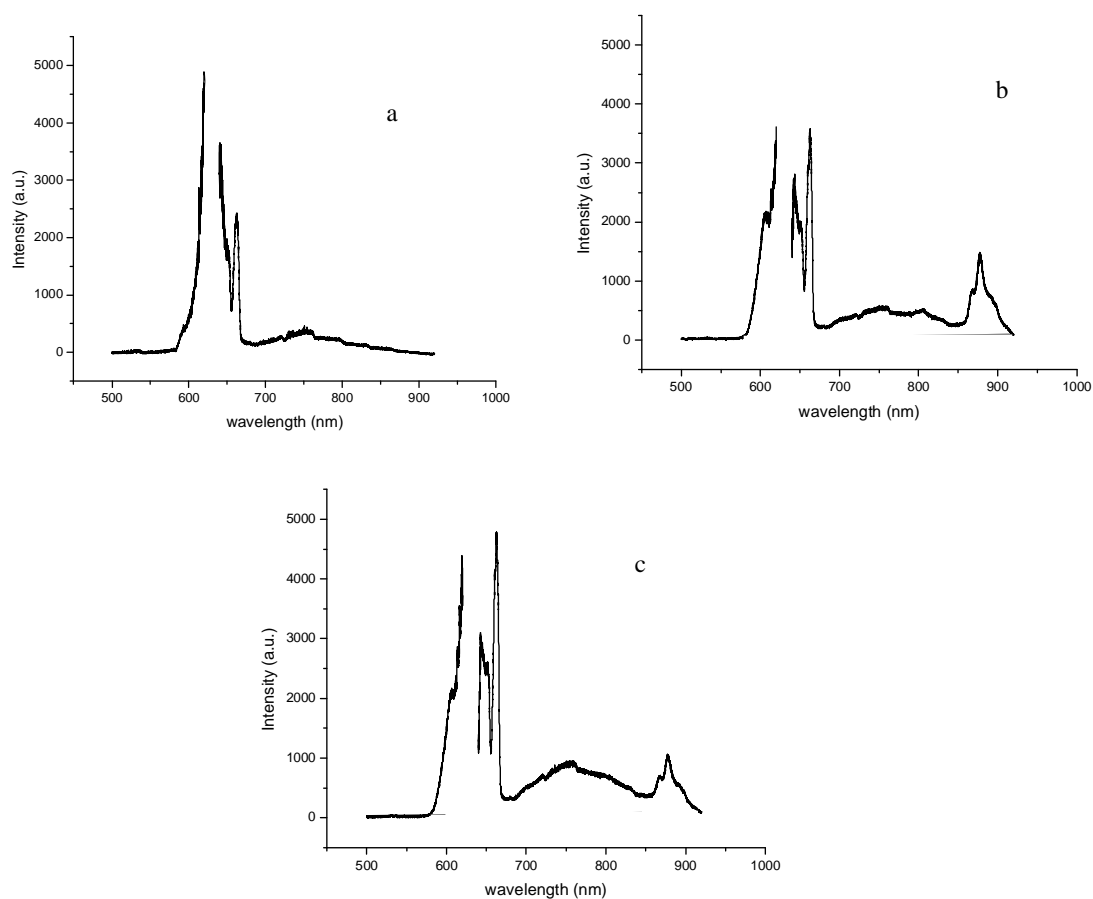

Fig. 3. Photoluminescence spectrum of a/ TPO, b/ TPO:1000 wt-ppm Pr^{3+},
c/ TPO:2000 wt-ppm Pr^{3+} glasses.
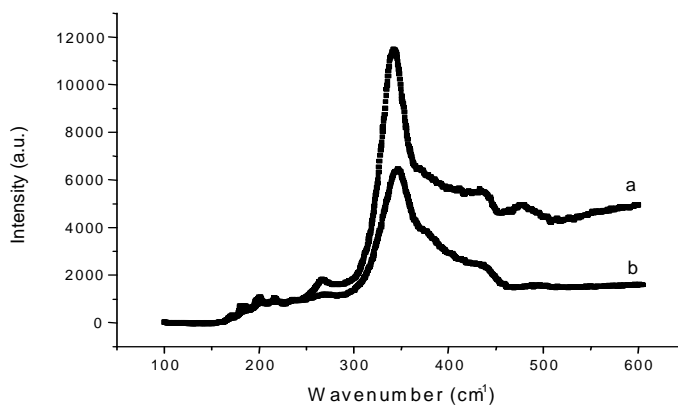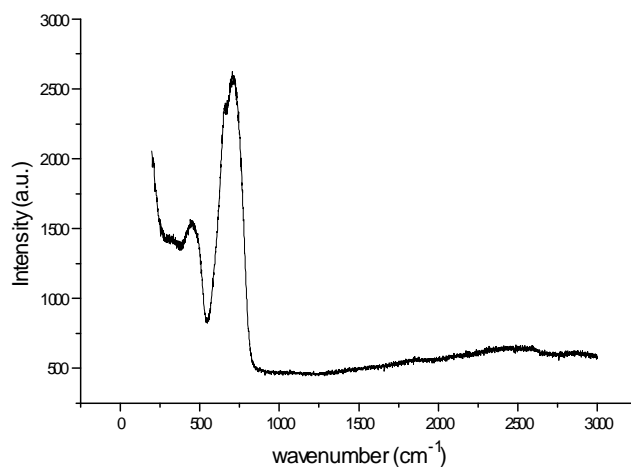

Fig. 4. Raman spectra of a/ GGS and b/ GAGS glasses.

Fig. 5. Raman spectrum of a TPO glass.

In Fig. 6 b, a thermogram of the $Ge_{25}Ga_{10}S_{65}$ glass doped with 3000 wt-ppm Pr^{3+} is presented. Upon doping, the glass transition temperature significantly decreases (T_g = 357.5 $^{\circ}$C). Because T_{ULS} = 446.3 $^{\circ}$C and T_x = 582 $^{\circ}$C, the doped glass has a broad region of the undercooled liquid state which is suitable for fiber drawing.
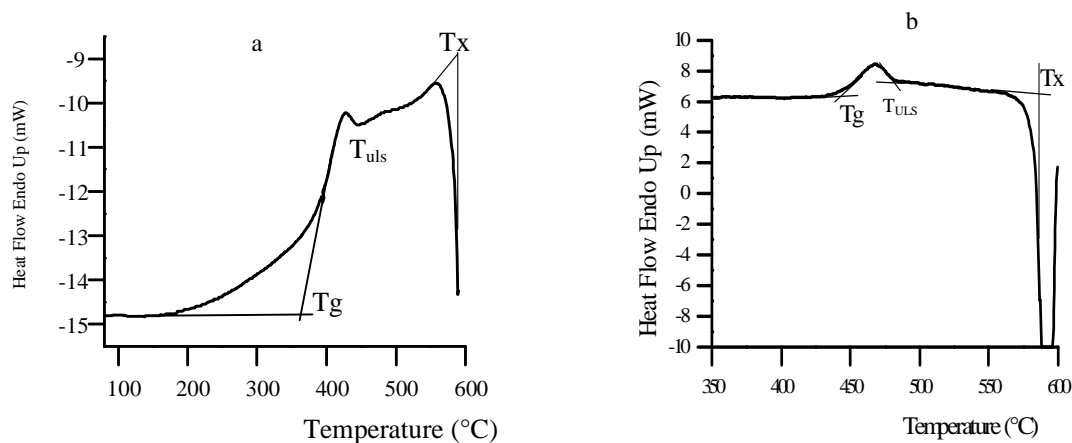

Fig. 6. a) DSC thermogram, first cycle (v = 40 $^{\circ}$ C/min) of the CGS glass doped with 3000 wt-ppm, b) Differential DSC thermogram of the GGS glass (v = 40 $^{\circ}$ C/min).

4. Discussion

4.1. Absorption spectra

Absorption spectra of both Ge-Ga-S and Ge-Ga-As-S glasses show that for Pr^{3+} doping, a pump band at 1.031 μm ($^3H_4 \rightarrow {}^1G_4$) is most convenient because their disturbing luminescence band at 1.075 μm is not excited by the Ti:Sapphire laser [3]. In TPO glasses doped with Pr^{3+}, dominant absorption bands are at 1.55, and 1.95 and 1.18 μm. We could not use them for excitation. In our next experiments we want to use a laser with a wavelength close to 460 nm.

4.2. Photoluminescence spectra

In Pr^{3+} doped glasses, the radiation transition $^1G_4 \rightarrow ^3H_5$ at 1.355 µm provides a possibility of using this glass for optical amplifying fibers. The Pr^{3+} ion quickly returns to the $^3H_4$ ground state by fast non-radiation decay. The Pr^{3+} ions represent a four-level amplifier system, although only three levels ($^3H_4$, $^1G_4$, $^3H_5$) are involved (Fig. 3d). In this system, $^1G_4$ state represents both the pump-excited state and metastable one. The non-radiative transition $^1G_4 \rightarrow ^3F_4$ competes with the radiation transition $^1G_4 \rightarrow ^3H_5$. Therefore, a low phonon energy host glass is necessary.

In our experiments both with GGS and with GAGS glasses, the 817-nm laser excited Pr^{3+} also to the $^1D_2$ state and ^3P manifolds and radiation transitions at 0.9 µm and at 1.08 µm were detected. In our experiments with TPO glasses, the 632.8 nm laser could excite only the strongest PL transition at 869/877 nm.

4.3. Raman spectra

In both GGS and GAGS glasses the peak at 340-345 cm^{-1} dominates. It can be assigned to A_1 vibrations of GeS_4 or GaS_4 tetrahedral groups. The peak at 240-265 cm^{-1} can be assigned to the S_3Ge-GeS_3 or S_3Ga-GaS_3 groups [11]. The peak at 435 cm^{-1} can be assigned to the S_3Ge-S-GeS_3 or S_3Ga-S-GaS_3 groups. The peak at 470-480 cm^{-1} can be assigned to a vibration mode of the S-S bonds [3]. A three-dimensional network of the four-fold coordinated germanium atoms and of the two-fold coordinated sulfur atoms is typical for germanium-sulfide glasses. Tetrahedral GeS_4 units are linked by edges and corners. In the Ge-Ga-S glass, gallium atoms prefer a tetrahedral environment (due to a small difference between atomic masses of Ge and Ga) and compete with germanium atoms as glass formers. At high concentrations of Ga atoms (20 m/o Ga_2S_3), due to a shortage of sulfur atoms, the formation of S_3Ga-GaS_3 structural units is observed [12]. The addition of the other glass former modifies the glass structure, and the number of GeS_4 tetrahedra, linked by edges, increases [3]. It seems that the formation of homopolar Ge-Ge bonds and edge shared GaS_4 tetrahedra is responsible for the increased solubility of rare earth ions in Ge-Ga-S glasses. By adding As_2S_3 only a small shift of the GaS_4 peak is observed. It seems that As atoms are 4-fold coordinated in these glasses.

A typical Raman spectrum of tellurite glasses is composed of three groups of modes at 550-850, 250-550 and 50-250 cm^{-1}, roughly corresponding to stretching, bending and torsional or rotational modes [13]. Our spectrum is very similar to that of 80 TeO_2•15 ZnO•5NaO [13]. In the range of 350-900 TeO_2•, it is rather identical to the spectrum of a TeO_2 glass [14], only the intensities of the peak above 700 cm^{-1} and of its shoulder at 659 cm^{-1} are interchanged. They all are assigned to the vibrations of the TeO_4 polyhedra. The only diference represents the peak at 320 cm^{-1} which can be probably assigned to Pb-Cl vibrations.

4.4. Phase transitions

The difference between T_x and T_g characterizes a stability of the glass against crystallization. For a satisfying drawing of glass fibers, this difference must exceed 80-100 $^{\circ}$C. The fiber drawing temperature lies usually in the upper part of the (T_g, T_x) interval and must be higher than T_{ULS}. At drawing temperature, the viscosity of the glass is about 10^7 Pa.s.

We have measured only the pure and doped GGS glasses as they seem to be most suitable for practical applications. In pure GGS glasses, the difference of T_x and T_g is sufficiently large as to allow fiber drawing. The doped glass has a broad region of the undercooled liquid state what is suitable for fiber drawing. The recommended temperature of fiber drawing is 510±30 $^{\circ}$C.

5. Conclusions

In the GGS and GAGS glasses doped with Pr^{3+} ions, seven absorption bands were detected in the spectral region of 200-3000 nm. The band at 1.031 µm ($^3H_4 \rightarrow ^1G_4$) is most convenient for pumping. In the TPO glass, only six absorption bands due to optical transitions from $^3H_4$ level of Pr^{3+}

ion have been detected. In comparison to sulfide glasses, these levels are significantly shifted to higher energies.

In the range of 800 nm to 1500 nm, three bands of the photoluminescence spectrum were found in both the GGS and GAGS glasses doped with Pr^{3+}. For optical amplifying, an excitation with Ti: Sapphire laser is most appropriate because the luminescence band at 1075 nm does not disturb.

In the TPO glass doped with Pr^{3+}, only the strongest luminescent band at 869/877 nm was found due to lack of a suitable laser in our laboratory.

Raman spectra confirmed homogeneity of GGS and GAGS glasses and indicated that the coordination of Ge, Ga and As is similar.

In TPO glasses, the Raman spectrum shows three bands assigned to the vibrations of the TeO_4 polyhedra and one which, probably, comes from the vibrations of the Pb-Cl bonds.

In pure and doped GGS glasses, the difference of T_x and T_g is sufficiently large as to allow fiber drawing. The doped glass has a broader region of the undercooled liquid state what is more suitable for the drawing. The recommended drawing temperature is $510\pm30\ ^oC$.

Acknowledgement

References

 [1] J. Lucas, Revue Phys. Appl. **21**, 683 (1986).
 [2] M. Poulain, Endeavour **11,** 25 (1987).
 [3] D. R. Simmons, Germanium gallium sulfide glasses for Pr-doped fiber amplifiers at 1.3 μm. Thesis, Eindhoven University of Technology, Eindhoven (1995).
 [4] D. Ležal, J. Optoelectron. Adv. Mater. **5,** 23 (2003).
 [5] S. H. Park, J. Heo, H. S. Kim, J. Non-Cryst. Solids **259,** 31 (1999).
 [6] D. Ležal, M. Poulain, J. Zavadil, Ceramics **45**, 105 (2001).
 [7] K. Wei, D. P. Machewirth, J. Wenzel, E. Snitzer, G. H. Sigel Jr., J. Non-Cryst. Solids **182**, 256 (1995).
 [8] D. Ležal, J. Pedlíková, J. Gurovič, R. Vogt, Ceramics **40**, 55 (1996).
 [9] D. Ležal, J. Pedlíková, P. Kostka, J. Bludska, M. Poulain, J. Zavadil, J. Non-Cryst. Solids **284,** 288 (2001).
[10] M. Ožvoldová, V. Trnovcová, O. Bošák, V. Kaššáková, D. Ležal, J. Greguš, V. Gašparík, E. Illeková, M. Kadlečíková, CO-MAT-TECH 2002, Trnava, Ed. K. Rešetová, Fac. Mater. Sci. & Technol. SUT, Trnava, Slovakia 2002, p. 100.
[11] B. G. Aitken, C. W. Ponader, J. Non-Cryst. Solids **256/257,** 143 (1999).
[12] V. Trnovcová, Czech. J. Phys. A **33**, (1983).
[13] S. Marjanovic, J. Toulouse, H. Jain, C. Sandmann, V. Dierolf, A. R. Kortan, N. Kopylov, R. G. Ahrens, J. Non-Cryst. Solids **322,** 311 (2003).
[14] B. Jeansannetas, S. Blanchandin, P. Thomas, P. Marchet, J. C. Champarnaud-Mesjard, T. Merle-Mejean, B. Frit, J. Solid State Chem. **146,** 329 (1999).